Journal of Agronomy and Crop Science

WILEY

Journal of Agronomy and Crop Science

ORIGINAL ARTICLE

Heat Stress

Integrating Curve-Shape Traits to Assess Photosynthetic Thermal Responses in Rice

Qiaoyun Zhang[1] | Sheng Liang[1] | Xianke Yang[1] | Xiaoxia Ling[1] | Liang Fang[2] | Dongliang Xiong[1]

[1]National Key Laboratory of Crop Genetic Improvement, Hubei Hongshan Laboratory, MARA Key Laboratory of Crop Ecophysiology and Farming System in the Middle Reaches of the Yangtze River, Huazhong Agricultural University, Wuhan, Hubei, China | [2]Department of Forestry, College of Forestry, Fujian Agriculture and Forestry University, Fuzhou, Fujian, China

Correspondence: Dongliang Xiong (dlxiong@mail.hzau.edu.cn)

Received: 30 December 2025 | **Revised:** 28 February 2026 | **Accepted:** 4 March 2026

Keywords: curve-shape traits | daily carbon gain | *Oryza* | photosynthetic thermal breadth | temperature

ABSTRACT

We examined whether conventional peak-based traits or curve-shape characteristics better explain photosynthetic performance under realistic warming conditions that combine elevated mean temperatures with pronounced diurnal fluctuations and recurrent heat extremes. Photosynthetic temperature-response curves of 14 rice genotypes, including wild relatives and cultivated varieties, were quantified using a unified modified Arrhenius model, and thermal breadth and sensitivity traits were extracted and used to simulate daily carbon gain under midsummer diurnal temperature patterns. All 14 genotypes exhibited substantial divergence in their photosynthetic thermal responses. While the optimum temperature for photosynthetic rate (T_{opt}) was highly conserved (the phenotypic coefficient of variation, PCV = 5.7%), shape-based metrics showed far greater variation, especially the high-temperature sensitivity ($Slope_{higher}$), with PCV exceeding 70%. Thermal breadth (Breadth80) ranged from 14.2°C to 29.1°C, and A_{opt} varied by more than 60% across genotypes. Then the genotypes were divied into distinct thermal response groups, which are broad-and-stable types (e.g., SY63, N22), high-capacity but fragile types (e.g., *O. glumaepatala* (E8-2)), and heat-sensitive types (e.g., LYPJ). Simulations revealed that daily carbon gain corresponded more strongly to Breadth80 and high-temperature sensitivity than to peak traits. Our findings demonstrate that thermostability, not peak performance, is the key determinant of carbon assimilation under hot environments with substantial daytime temperature fluctuations. Incorporating curve-shape traits into breeding and phenotyping efforts will be essential for developing climate-resilient rice.

1 | Introduction

Global warming and its impacts on regional agroecosystems are becoming increasingly pronounced (Gong et al. 2023; Jagadish et al. 2014; Xu et al. 2020; Liu et al. 2018; Mathur et al. 2014; Shi et al. 2017; Xu et al. 2020). In the middle reaches of the Yangtze River, a core rice-producing region characterised by a subtropical monsoon climate, summer temperatures during the rice growing season have risen markedly in recent decades (Deng et al. 2023; Li et al. 2025; Liu et al. 2024). Daytime air temperatures in July and August now commonly remain above 30°C, with extreme events frequently approaching or exceeding 40°C (CMA 2024). These conditions indicate a shift toward high temperatures that are not only more intense, but also more persistent and recurrent (Jiang et al. 2023, 2024; Radhakrishna et al. 2018). In addition to elevated means, the region typically experiences diurnal temperature ranges of around 10°C, exposing rice plants to substantial thermal fluctuations within a single day (Rehmani et al. 2021; Sang 2012; Yang, Zhang, Li, et al. 2020; Zhang et al. 2025). Therefore, understanding how rice photosynthesis responds to both high temperatures and their fluctuations has become essential for anticipating the impacts of future climate warming on regional rice production (Kanno et al. 2009; Makino 2021).

Key Points

- Traditional peak photosynthesis metrics poorly predict rice performance in fluctuating high temperatures.
- Photosynthetic thermal stability shows great genetic variation, captured by curve-shape traits.
- Daily carbon gain is governed more by thermal breadth than by peak photosynthetic capacity.
- Curve-shape traits provide a novel phenotyping toolkit for breeding climate-resilient rice.

The response of photosynthesis to temperature has long been recognised as one of the central questions in plant ecophysiology (Angilletta 2006; Asbury and Angilletta 2010; Kontopoulos et al. 2024; Molnár et al. 2017). It is now well established that the relationship between net photosynthetic rate and leaf temperature is not linear but follows a characteristic unimodal pattern, typically represented by a peaked curve (Atkin et al. 2006; Bernacchi et al. 2003; Bytnerowicz et al. 2022; Dusenge et al. 2025; Mathur et al. 2014; Medlyn et al. 2002; Padfield et al. 2021; Sage and Kubien 2007; Salvucci and Crafts-Brandner 2004; Sharkey 2005; Sharkey and Zhang 2010; Way and Yamori 2013; Yamasaki et al. 2002; Yamori et al. 2013; Yamori et al. 2005). Among the various analytical frameworks developed, Arrhenius-type models, particularly modified formulations incorporating enzyme deactivation at high temperatures, have become the common tools for quantifying photosynthetic thermal responses (Mathan et al. 2021; Medlyn et al. 2002; Molnár et al. 2017; Noguchi et al. 2015; Yin 2021), although debate exists (Kontopoulos et al. 2024; Padfield et al. 2021). These models capture the fundamental biochemical processes that govern temperature-dependent changes in photosynthetic capacity and allow the estimation of key peak parameters such as the optimal temperature for photosynthesis (T_{opt}) and the maximum photosynthetic rate (A_{opt}) (Geange et al. 2020; Glaubitz et al. 2014; Moore et al. 2021; Yamori et al. 2005, 2013; Yang, Zhang, Huang, et al. 2020).

However, the peak-centric perspective presents important limitations when extrapolated to field conditions (Sharkey 2005). T_{opt} often shows strong conservatism and limited plasticity across species (Crous et al. 2024; Dusenge et al. 2021; Wittemann et al. 2022), making it unlikely to fully track rising environmental temperatures. Moreover, crop performance depends not solely on behaviour at the thermal optimum but on the ability of photosynthesis to be sustained as temperatures fluctuate around and depart from that optimum (Cai et al. 2020; Song et al. 2019; Yin and Struik 2017).

A growing body of work suggests that the shape of the thermal response curve—including its symmetry, breadth and rates of decline on either side of T_{opt}—may be equally or even more important under fluctuating thermal environments (Dowd et al. 2015; Dusenge et al. 2025; Rohr et al. 2018). Two genotypes may share similar A_{opt} values yet differ markedly in thermal sensitivity, that one may display a narrow, sharply peaked curve that declines steeply with modest warming, whereas another may exhibit a broader, more plateau-like curve that maintains moderate rates over a wider temperature range (Briceño et al. 2025; Carter et al. 2019; Rohr et al. 2018). Under natural conditions, where leaf temperatures rarely remain at T_{opt} for extended periods (Liu et al. 2025), genotypes with modest peaks but broad, stable curves may accumulate more carbon over the day than those with higher but fragile peaks (Busch et al. 2007; Galmés et al. 2015; Katahata et al. 2014; Way and Sage 2008). These insights highlight the need to move beyond traditional peak-centric assessments and to incorporate curve-shape characteristics in order to more accurately capture physiological performance under realistic fluctuating temperatures.

In the present study, we investigated photosynthetic temperature-response curves of 14 genetically diverse rice accessions, and quantified both peak-related traits and shape-based traits that describe performance breadth and thermal sensitivity. Our objectives were: (1) to characterise the extent and pattern of genetic variation in both peak-related traits and shape-based traits across rice genotypes; and (2) to assess how different combinations of peak and shape-based traits influence daily carbon assimilation estimation under realistic diurnal temperature fluctuations.

2 | Materials and Methods

2.1 | Plant Materials and Growth Conditions

To explore the natural variation in photosynthetic responses to temperature, we studied 14 genotypes representing wide diversity in species, geographical origin and variety. These included six wild relatives: *O. alta* (E1-6), *O. grandiglumis* (E6-3), *O. glumaepatala* (E8-2 and E8-3), *O. latifolia* (E9-4) and *O. subulata* (E21-1), and eight cultivated varieties of *O. sativa*: Huanghuazhan (HHZ), Shanyou63 (SY63), Yangliangyou 6 (YLY6), Yangdao 6 (YD6), Liangyoupeijiu (LYPJ), Nagina 22 (N22), Nangeng 9108 (NG9108) and Yongyou 12 (YY12) (Table S1). Rice seedlings were transplanted into 3-L pots filled with dry paddy soil, with each pot containing three hills. All plants were grown outdoors on the campus of Huazhong Agricultural University. A total of 6.0 g of compound fertiliser (N:P_2O_5:K_2O = 15:15:15) was applied: 3.0 g as a basal application and the remaining 3.0 g applied at the early tillering stage, 10 days before gas-exchange measurements commenced. To mitigate disease and pest pressure, pesticides were applied 15 days after transplanting and again 7 days before gas-exchange measurements. Measurements were conducted on the youngest fully expanded leaves at the late tillering stage.

2.2 | Gas Exchange Measurements

Gas exchange was measured using a portable photosynthesis system (LI-6800-01, LI-COR Inc., USA), equipped with a 2 cm^2 integrated fluorescence chamber head. Measurements were performed between 08:00 and 17:30 in a walk-in growth chamber (GR48, Conviron, Canada). Temperature response curves were constructed by measuring the net photosynthetic rate (A_n) across a series of controlled leaf temperatures (T_{leaf}).

Before measurements commenced, the walk-in growth chamber was set to 30°C, and allowed to reach thermal equilibrium.

Once stabilised, six seedling pots of were randomly selected and transferred from outdoors into the chamber, where they acclimated for at least 30 min (Bytnerowicz et al. 2022; Coast et al. 2021). During this interval, the LI-6800-01 was also placed inside the chamber and its T_{leaf} setting was adjusted to match the ambient chamber temperature. In each pot, a youngest fully expanded leaf was identified and marked, and all gas exchange measurements at different T_{leaf} were taken from this same leaf. The PPFD, CO_2 concentration, flow rate, fan speed and leaf-to-air vapour pressure deficit (VPD) in the gas exchange chamber were set at 1500 $\mu mol\, m^{-2} s^{-1}$, 400 $\mu mol\, mol^{-1}$, 300 $\mu mol\, s^{-1}$, 10,000 rpm and 1.5 kPa, respectively.

The measurement sequence started at a T_{leaf} of 30°C. After the leaf equilibrated to the gas exchange chamber conditions (the fluctuation of A_n was less than 2% in 2 min), the gas exchange data were recorded. Subsequently, both growth-chamber temperature and the T_{leaf} of LI-6800-01 settings were adjusted to the next target temperature in the sequence. Seedlings and the instrument were then allowed at least 20 min to re-equilibrate before measurements resumed.

The full target temperature sequence was 30°C, 35°C, 40°C, 30°C, 25°C, 20°C and 15°C. Once the gas exchange measurements finish above 30°C of T_{leaf}, the growth chamber and leaf temperature were set back to 30°C before proceeding to lower temperatures. For each genotype, four to six independent biological replicates were measured.

2.3 | Temperature Response Curve Fitting

The temperature response curve of the net photosynthetic rate (A_n) is fitted to the modified Arrhenius model (Medlyn et al. 2002), which describes temperature-dependent biochemical rates by combining an Arrhenius increase at low temperatures with a deactivation term that reduces rates at high temperatures due to enzyme instability, quantified through a deactivation energy (D_s; J mol^{-1}) and an entropy term (S_s; J $mol^{-1} K^{-1}$) that together determine the sharpness and position of the decline. The equation of the model is given by:

$$A_n = A_{25} \exp\left[\frac{E_a}{R}\left(\frac{1}{298} - \frac{1}{T_{leaf}}\right)\right]\left(\frac{1+\exp\left[\frac{D_s}{R}\left(\frac{S_s}{D_s} - \frac{1}{298}\right)\right]}{1+\exp\left[\frac{D_s}{R}\left(\frac{S_s}{D_s} - \frac{1}{T_{leaf}}\right)\right]}\right) \quad (1)$$

where A_{25} is the photosynthetic rate at T_{leaf} = 25°C, E_a, D_s and S_s (J mol^{-1}) are the activation energy, deactivation energy and the entropy factor, respectively, and R is the universal gas constant (8.314 J $mol^{-1} K^{-1}$).

To estimate the optimal photosynthetic rate (A_{opt}) and the temperature at which this maximum occurs (T_{opt}), Equation (1) was re-parameterised following Medlyn et al. (2002). The reformulated expression takes the following form:

$$A_n = A_{opt} \frac{D_s \exp\left[\frac{E_a}{R}\left(\frac{1}{T_{opt}} - \frac{1}{T_{leaf}}\right)\right]}{D_s - E_a\left\{1 - \exp\left[\frac{D_s}{R}\left(\frac{1}{T_{opt}} - \frac{1}{T_{leaf}}\right)\right]\right\}} \quad (2)$$

2.4 | Deriving Thermal Breadth and Sensitivity Traits From Fitted Curves

The interpretation of key parameters derived from representative photosynthetic temperature-response curves is illustrated in Figure 1. As illustrated in Figure 1A,B and Figure S1, the pair of parameters E_a and D_s jointly determine the overall shape of the response curve. A high E_a yields a steep rise in A_n prior to the T_{opt} (pre-T_{opt} region), whereas a high D_s leads to a sharp decline afterward (post-T_{opt} region). Consequently, combinations of large E_a and large D_s yield a narrow, sharply peaked curve, while smaller values generate broader, flatter thermal responses.

To quantify the genetic variation in thermal response beyond the shape parameters E_a and D_s, two additional metrics were also extracted from the fitted curves. First, the thermal photosynthetic breadth (Breadth80) was defined as the temperature range over which A, remains ≥ 80% of A_{opt} (Figure 1C, green solid line). It was calculated as Breadth80 = $T_{higher} - T_{lower}$, where T_{lower} and T_{higher} are the temperatures at which $A(T) = 0.8A_{opt}$. Second, temperature-sensitivity slopes ($Slope_{lower}$ and $Slope_{higher}$) were calculated to characterise how rapidly photosynthesis declines on either side of T_{opt}. $Slope_{lower}$ is the average rate of change in A_n between T_{lower} and T_{opt}, whereas $Slope_{higher}$ is the corresponding average rate between T_{opt} and T_{higher} (Figure 1C, blue and red segments). We used the chord-slope method ($\Delta A_n / \Delta T_{leaf}$) between these endpoints, which captures the overall decline pattern while reducing sensitivity to noise in the fitted curves compared with instantaneous derivatives.

For integrated comparison of thermal adaptation among genotypes, $Slope_{80}$ was expressed as the absolute values of $Slope_{lower}$ and $Slope_{higher}$ at the 80% A_{opt} thresholds. These two absolute slope values were combined as a holistic measure that complements Breadth80 and enables comparison of adaptation across the full temperature range.

2.5 | Simulation-Based Analysis of Daily Carbon Accumulation

Daily photosynthetic carbon gain was simulated to examine how different temperature-response characteristics influence carbon assimilation under realistic summer conditions. Photosynthesis was modelled assuming that leaf temperature equaled ambient air temperature. The response of A_n to photosynthetic photon flux density (PPFD) was described using the non-rectangular hyperbola model of Du et al. (2020), parameterised for rice (quantum yield = 0.05, convexity = 0.85, dark respiration = 1.0 $\mu mol\, m^{-2} s^{-1}$, maximum gross photosynthetic rate = 35 $\mu mol\, m^{-2} s^{-1}$). This light-response formulation represents instantaneous A_n–PPFD relationships and does not account for circadian or other environmental factors (e.g., VPD).

The simulation comprised two ways. First, a theoretical analysis was conducted using two representative temperature-response curve types, chosen to illustrate contrasting thermal photosynthetic profiles. For this analysis, we constructed a typical midsummer diurnal course by averaging all air

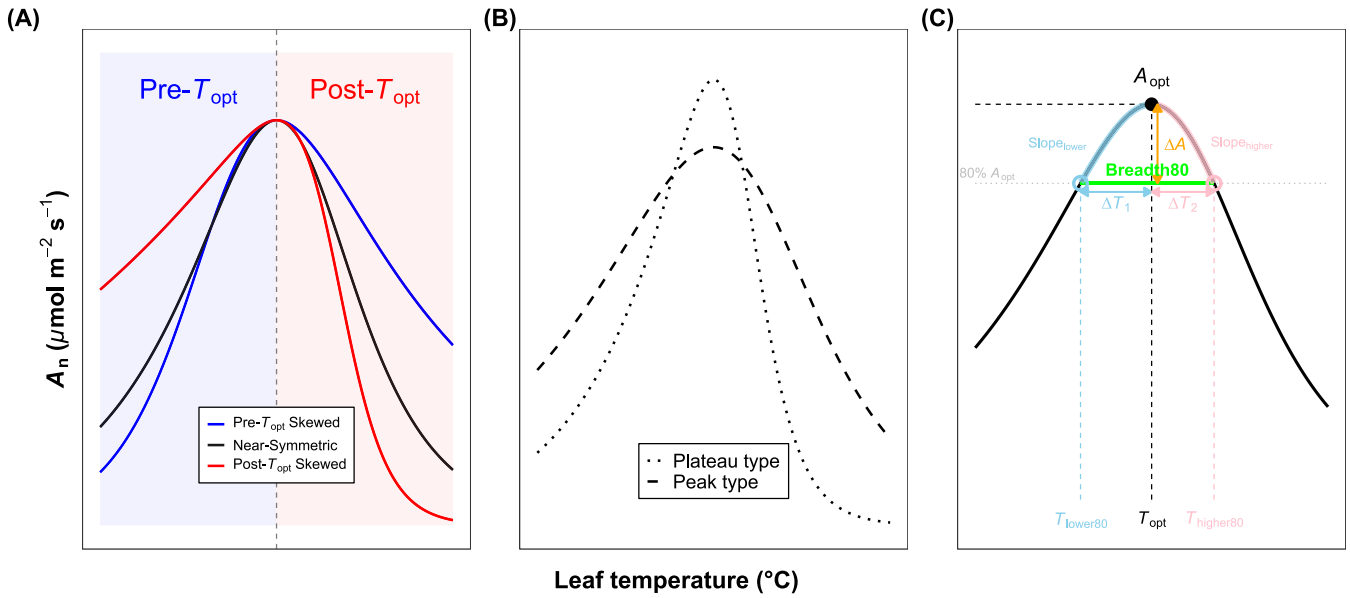

FIGURE 1 | Conceptual illustration of photosynthetic temperature response curve shapes and derived thermal traits. (A) Examples of three contrasting thermal response curve shapes relative to the optimum temperature (T_{opt}). Curves differ in the degree of asymmetry around T_{opt}, a pre-T_{opt}–skewed curve (blue) shows a gradual rise and steeper decline, a near-symmetric curve (black) shows similar rates of increase and decrease, and a post-T_{opt}–skewed curve (red) shows a steep rise followed by a gradual decline. Shaded regions indicate the pre-T_{opt} (blue) and post-T_{opt} (red) portions of the curve. (B) Illustration of two representative curve types highlighting differences in overall shape, a plateau type curve (dotted line), characterised by a broad, flat region around T_{opt} and a peak type curve (solid line), characterised by a narrow, sharply defined maximum. (C) Schematic showing the extraction of key shape-based thermal traits from a fitted temperature-response curve. Thermal breadth (Breadth80) is defined as the temperature range over which the photosynthetic rate (A_n) remains ≥80% of A_{opt} (green segment). $T_{lower80}$ and $T_{higher80}$ mark the lower and upper temperatures at the 80% threshold. Pre-T_{opt} and post-T_{opt} temperature sensitivities (Slope$_{lower}$ and Slope$_{higher}$) are calculated as the average rates of change ($\Delta A_n/\Delta T_{leaf}$) between $T_{lower80}$–T_{opt} and T_{opt}–$T_{higher80}$, respectively. Specifically, Slope$_{lower}$ = $\Delta A_n/\Delta T_{leaf1}$ and Slope$_{higher}$ = $\Delta A_n/\Delta T_{leaf2}$, corresponding to the blue and red segments.

temperature and PPFD measurements recorded in Wuhan during August 2025 at each 10-min time of day. These averaged diurnal patterns were used as environmental inputs to evaluate how the two representative curve shapes differ in potential daily carbon gain.

Second, daily carbon gain was simulated for all 14 rice genotypes using environmental data from a single representative clear day in August 2025 (Figure S4). This day was selected for its typical high-temperature features: temperature ranged from approximately 29°C to 35°C (a fluctuation of about 6°C), and maximum light intensity was approximately 1300 μmol m^{-2} s^{-1}. Air temperature and PPFD were measured every 10 min from 06:00 to 18:00, and these values were combined with each genotype's fitted temperature-response curve and the Du light-response model to compute A_n at each time step. Daily photosynthetic carbon gain was then obtained by numerically integrating A_n across the 12-h daytime period. This approach allowed direct comparison among genotypes under a realistic summer diurnal environment while separating theoretical curve-shape analysis from genotype-specific performance estimation.

2.6 | Statistical Analysis

Differences in measured traits among species were assessed using one-way analysis of variance (ANOVA), and pairwise comparisons were performed with Tukey's HSD test at a significance level of $\alpha = 0.05$, implemented using the *multcomp* package. Trait–trait relationships were examined using the standardised axis (SMA) regression with the *smatr* package. Phenotypic variance (PV) and phenotypic coefficient of variance (PCV) for temperature response parameters were calculated following Acevedo-Siaca et al. (2021). PV represents the average squared deviation from the mean, whereas PCV equals the standard deviation divided by the mean. All statistical analyses were conducted in R version 4.2.2 (R Core Team 2022).

3 | Results

3.1 | Genetic Variation in Photosynthetic Thermal Response

The photosynthetic rate at given leaf temperatures varied significantly among genotypes (Figure 2A). At 25°C, the highest A_n was observed in *O. glumaepatala* (E8-2) (30.1 ± 1.4 μmol m^{-2} s^{-1}) and the lowest in *O. latifolia* (E9-4) (17.3 ± 1.1 μmol m^{-2} s^{-1}), representing a 1.7-fold difference (Table S2). Below 25°C, the maximum A_n was recorded in HHZ at 20°C (23.9 ± 1.8 μmol m^{-2} s^{-1}), while the minimum in YY12 (12.9 ± 1.8 μmol m^{-2} s^{-1}), yielding a difference of 11 μmol m^{-2} s^{-1}. Above 25°C, *O. glumaepatala* (E8-2) consistently exhibited the highest A_n: 35.0 ± 0.6 μmol m^{-2} s^{-1} at 30°C and 33.4 ± 1.1 and 32.9 ± 1.0 μmol m^{-2} s^{-1} at 35°C and

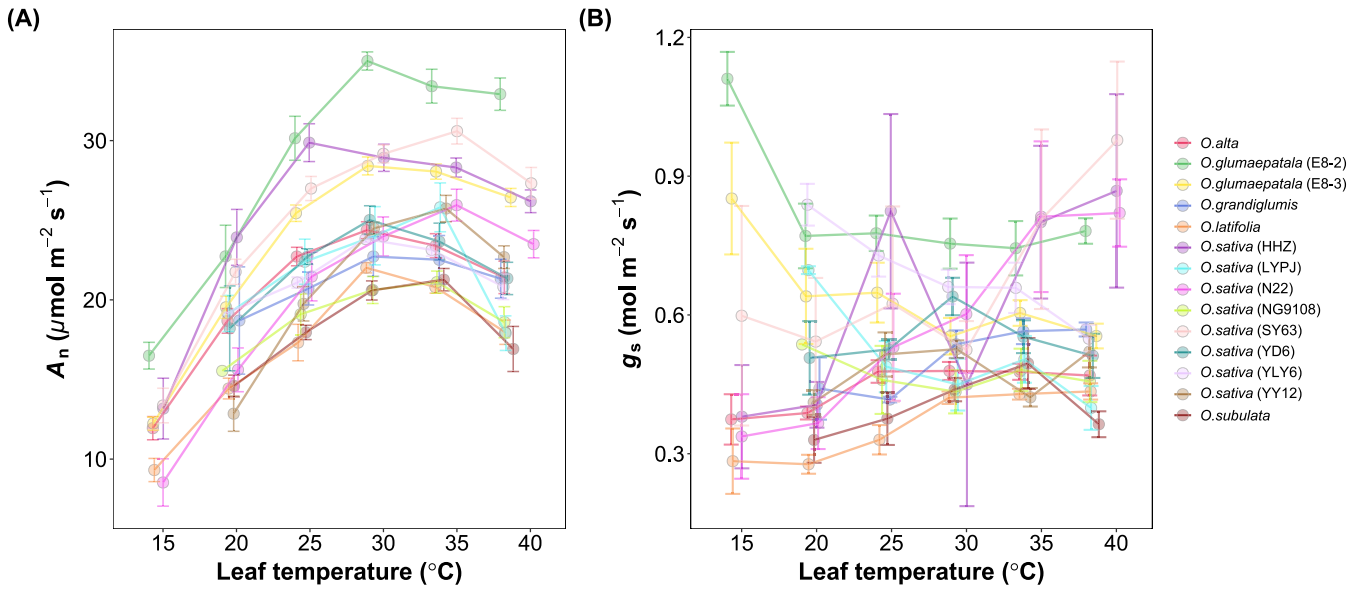

FIGURE 2 | Genetic variation in photosynthetic and stomatal responses to leaf temperature among 14 rice genotypes. (A) Net photosynthetic rate (A_n) measured across seven leaf temperatures (15°C–40°C). (B) Stomatal conductance (g_s) measured across the same temperature series. Error bars represent ± SE ($n = 4–6$).

40°C, respectively. In contrast, the lowest A_n at these temperatures occurred in *O. subulata* (E21-1) (20.6 ± 0.6 μmol m^{-2} s^{-1} at 30°C; 16.9 ± 1.4 μmol m^{-2} s^{-1} at 40°C) and *O. latifolia* (E9-4) (20.8 ± 0.4 μmol m^{-2} s^{-1} at 35°C), resulting in maximum differences of 14.4, 12.6 and 16.0 μmol m^{-2} s^{-1}, respectively.

Overall, genotypic variation in A_n was more pronounced above 25°C than below it, indicating genotype-specific differences in thermal sensitivity. The temperature threshold for the onset of photosynthetic decline also varied: HHZ exhibited the lowest (onset near 25°C), while N22 showed the highest (onset around 35°C), and the remaining genotypes fell between these two extremes. In contrast to the clear temperature-dependent variation observed in A_n, stomatal conductance (g_s) exhibited no consistent pattern across temperatures or genotypes, with any genotype-specific changes being minor and less variable than those in A_n (Figure 2B).

3.2 | Temperature-Response Curve Shape and Derived Thermal Parameters

While all genotypes exhibited a unimodal temperature response, the shapes of their photosynthetic curves varied markedly in both the rising and declining phases (Figure 3). Below T_{opt}, genotypes differed in how rapidly photosynthetic rates increased with warming, ranging from steep surges (e.g., HHZ, YY12) to more gradual rises in others. Above T_{opt}, variation was more pronounced, with some genotypes showing sharp declines (e.g., LYPJ, *O. subulata* (E21-1)) and others maintaining gradual decreases.

These contrasting curve shapes were further quantified by the derivatives of the fitted curves (Figure 3), confirming substantial genotypic differences in thermal sensitivity both before and after T_{opt}. HHZ showed the steepest pre-T_{opt} increase ($Slope80_{lower} = 0.81$, $Slope50_{lower} = 1.33$), indicating strong photosynthetic stimulation by warming. Conversely, LYPJ exhibited the steepest post-T_{opt} decline ($Slope80_{higher} = 1.42$, $Slope50_{higher} = 2.41$), reflecting the highest heat sensitivity.

Genetic variation was substantial across all fitted photosynthetic temperature response parameters (Tables S3 and S4, Figure 4A and Figure S2). *O. glumaepatala* (E8-2) had the highest A_{opt} (34.82 ± 0.80 μmol m^{-2} s^{-1}) and *O. latifolia* (E9-4) the lowest (21.32 ± 0.51 μmol m^{-2} s^{-1}). T_{opt} generally ranged 30°C–33°C, except for HHZ (27.22°C ± 0.78°C) and LYPJ (33.97°C ± 0.50°C). Breadth80 varied widely, from 14.17°C ± 0.80°C in E21-1 to 29.1°C ± 3.84°C in HHZ. Genotypic variation was greater in post-T_{opt} slopes (4.6-fold for $Slope80_{higher}$; 8-fold for $Slope50_{higher}$) than in pre-T_{opt} slopes (1.8-fold and 3.1-fold, respectively).

This genotypic variation was further quantified by phenotypic coefficient of variation (PCV, Figure 4A). T_{opt} showed the lowest PCV (5.7%), indicating relative conservation, while the post-T_{opt} slope exhibited the highest (70.6%), highlighting strong divergence in high-temperature sensitivity. Response asymmetry, measured as the pre-/post-T_{opt} slope ratio ($slope\_ratio_{80}$), clearly distinguished genotypes (Figure 4B): most (e.g., HHZ, 2.87) displayed a pre-T_{opt} bias (ratio > 1), whereas a minority (e.g., LYPJ, 0.32) showed a post-T_{opt} bias (ratio < 1). The coordination between pre- and post-T_{opt} sensitivities was threshold-dependent (Figure 4C and Figure S3), with a significant correlation at the 50% performance threshold but none at 80%, indicating performance-level-specific regulation of thermal sensitivity.

3.3 | Trait-Space Patterns of Photosynthetic Thermal Response

To visualise how genotypes differ in photosynthetic thermal response, we plotted thermal breadth (Breadth80) against

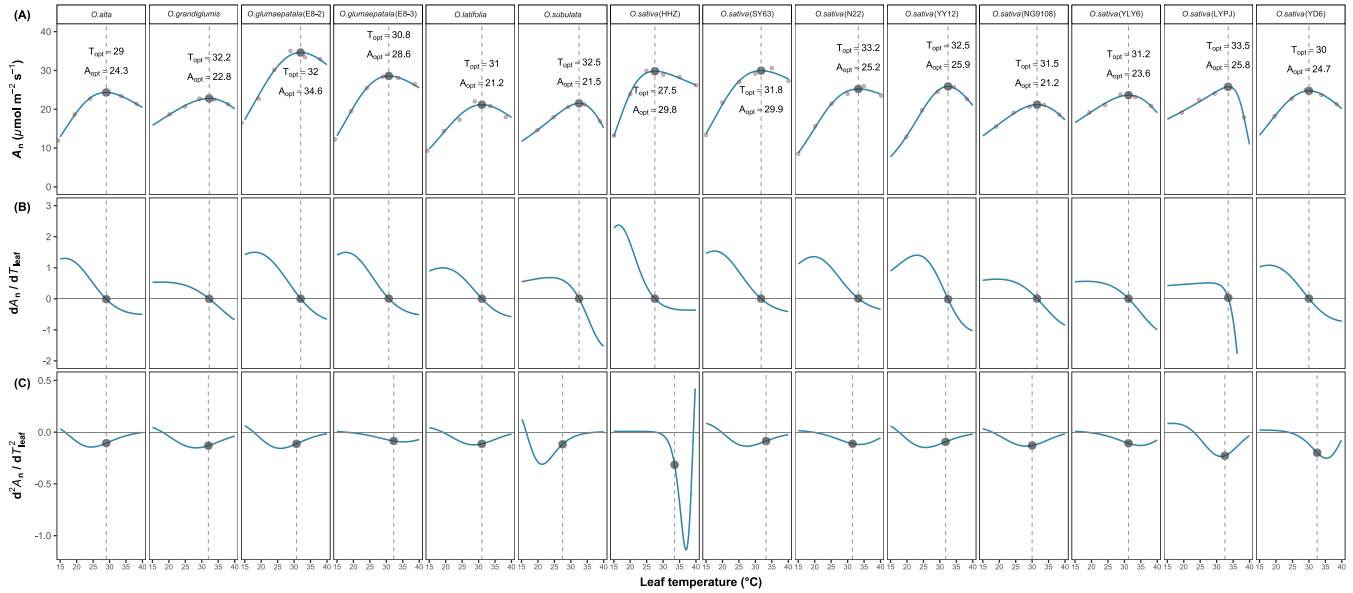

FIGURE 3 | Fitted photosynthetic temperature-response curves and their derivatives for 14 rice genotypes. (A) Fitted temperature-response curves of net photosynthetic rate (A_n) based on the modified Arrhenius model. The estimated optimum temperature (T_{opt}) and maximum photosynthetic rate (A_{opt}) are displayed within each panel. (B) First derivatives (dA_n/dT_{leaf}), representing the instantaneous rate of change in A_n with leaf temperature. These curves quantify the thermal sensitivity on either side of Topt and highlight genotypic differences in pre- and post-T_{opt} responses. (C) Second derivatives (d^2A_n/dT^2_{leaf}), capturing changes in curvature and identifying regions of acceleration and deceleration in thermal response.

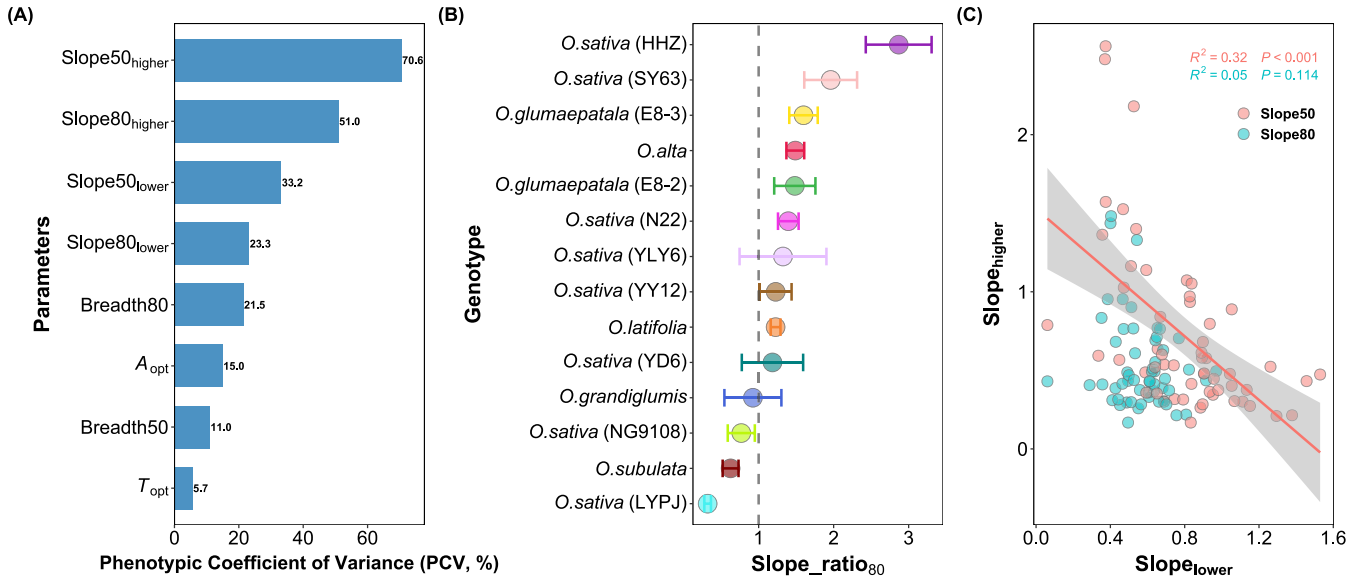

FIGURE 4 | Genetic variation and coordination among thermal response parameters. (A) Phenotypic coefficient of variation (PCV, %) for key photosynthetic thermal parameters; (B) Genotypic variation in response asymmetry, expressed as the ratio of pre-T_{opt} to post-T_{opt} slopes at the 80% A_{opt} threshold (Slope_ratio$_{80}$). Values > 1 indicate steeper stimulation below T_{opt} than decline above it; values < 1 reflect greater high-temperature sensitivity. Genotypes are ranked from most to least symmetric; and (C) Relationship between slope$_{lower}$ and slope$_{higher}$. Red and blue points represent values derived from 50% and 80% performance thresholds, respectively.

overall temperature sensitivity, quantified as the combined absolute slopes at the 80% A_{opt} points (Figure 5). The 14 genotypes occupied a broad continuum across this two-dimensional trait space, revealing clear contrasts in thermal response. The highly temperature-sensitive genotype LYPJ clustered in the narrow Breadth80–high Slope80 region, consistent with its steep decline in photosynthesis around T_{opt}. In contrast, SY63 and N22, both exhibiting large Breadth80 values and low Slope80, fell into the wide breadth–low sensitivity quadrant.

The A_{opt} gradients were also evident across the trait space. Genotypes with the highest A_{opt} values were concentrated toward the upper right, where large thermal breadth co-occurred with high temperature sensitivity. In contrast, genotypes with low absolute Slope80, those most tolerant of temperature fluctuations, were clustered toward the lower-right quadrant. In addition, correlation analysis revealed that genotypes with exceptionally high photosynthetic capacity tended to exhibit sharper declines away from their optimum, whereas highly stable genotypes generally had more moderate A_{opt}.

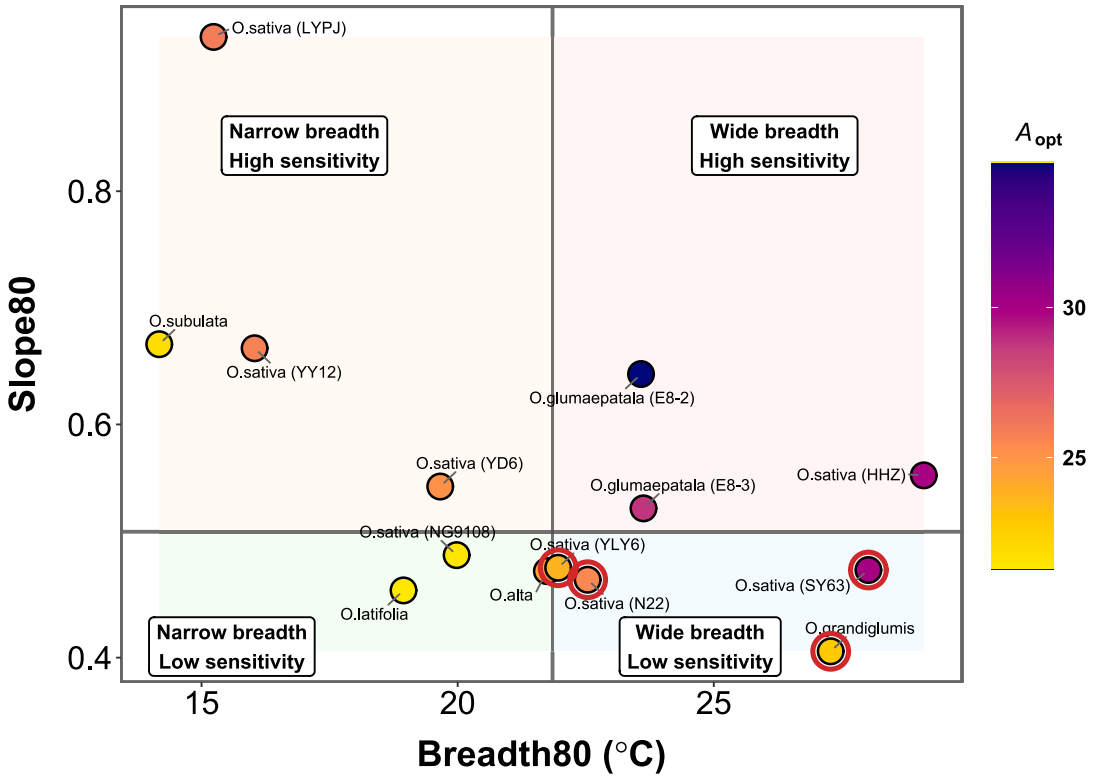

FIGURE 5 | Trait-space visualisation of thermal breadth and temperature sensitivity across 14 rice genotypes. Each point represents a genotype, plotted by its thermal breadth (Breadth80) and overall temperature sensitivity (Slope80). Solid grey lines indicate the median values of each trait, dividing the space into narrow breadth–high sensitivity (upper left, light-yellow background), wide breadth–high sensitivity (upper right, light-red background), narrow breadth–low sensitivity (lower left, light-green background) and wide breadth–low sensitivity (lower right, light-blue background). Point colours represent A_{opt} (higher values shown in deeper purple).

3.4 | Daily Photosynthetic Carbon Gain

To illustrate how temperature-response curve shapes affect carbon assimilation, we first compared two representative curve types (Figure 6A). Simulated under an averaged mid-summer diurnal course (constructed from August 2025 measurements; see Materials and Methods), the peak-type curve showed a sharp photosynthetic maximum near T_{opt} but declined rapidly when temperatures exceeded the optimum (Figure 6B,C). In contrast, the plateau-type curve maintained relatively stable, high photosynthetic rates across the daytime temperature range, resulting in substantially greater daily carbon accumulation (Figure 6D).

Building on this analysis framework, we next quantified daily carbon gain for all 14 genotypes using environmental data from a representative clear day in August 2025. The resulting genotypic differences were consistent with expectations based on Breadth80, Slope80 and A_{opt} (Figure 7 and Figure S5). Under identical natural fluctuations of temperature and light (Figure 7A), genotypes exhibited distinct diurnal patterns that differed in peak magnitude, duration of high activity and resilience to afternoon stress. These dynamic differences directly translated into a wide range of integrated daily carbon gain, as evidenced by the clear ranking of genotypes (Figure 7B). This demonstrates that genetic variation critically shapes not only instantaneous photosynthetic performance but, more importantly, the cumulative carbon productivity under realistic field conditions.

Genotype *O. glumaepatala* (E8-2) represented a high-performance type, exhibiting the greatest daily carbon gain. Its superior performance was driven by the combination of a high A_{opt} and broad thermal breadth, which enabled robust photosynthesis across variable daytime temperatures despite its relatively high temperature sensitivity (Tables S3 and S4). In contrast, LYPJ represented a temperature-sensitive type with the lowest daily carbon accumulation. Although its A_{opt} was not the lowest, its narrower thermal breadth and greater sensitivity beyond T_{opt} caused photosynthesis to decline more rapidly once a critical temperature threshold was exceeded, leading to significantly reduced carbon gain.

4 | Discussion

4.1 | Genetic Variation and Limitations of Peak-Based Thermal Traits

Our study revealed substantial genetic variation in the photosynthetic temperature responses of the 14 diverse genotypes. Differences in A_n were evident across the entire temperature range, with variation becoming particularly pronounced above 25°C, where heat sensitivity diverged sharply among genotypes. To allow consistent comparison across this diverse panel, we used the modified Arrhenius model (Medlyn et al. 2002), which provided a unified framework for quantifying both peak parameters and curve-shape characteristics across genotypes. This model effectively explains plant temperature response

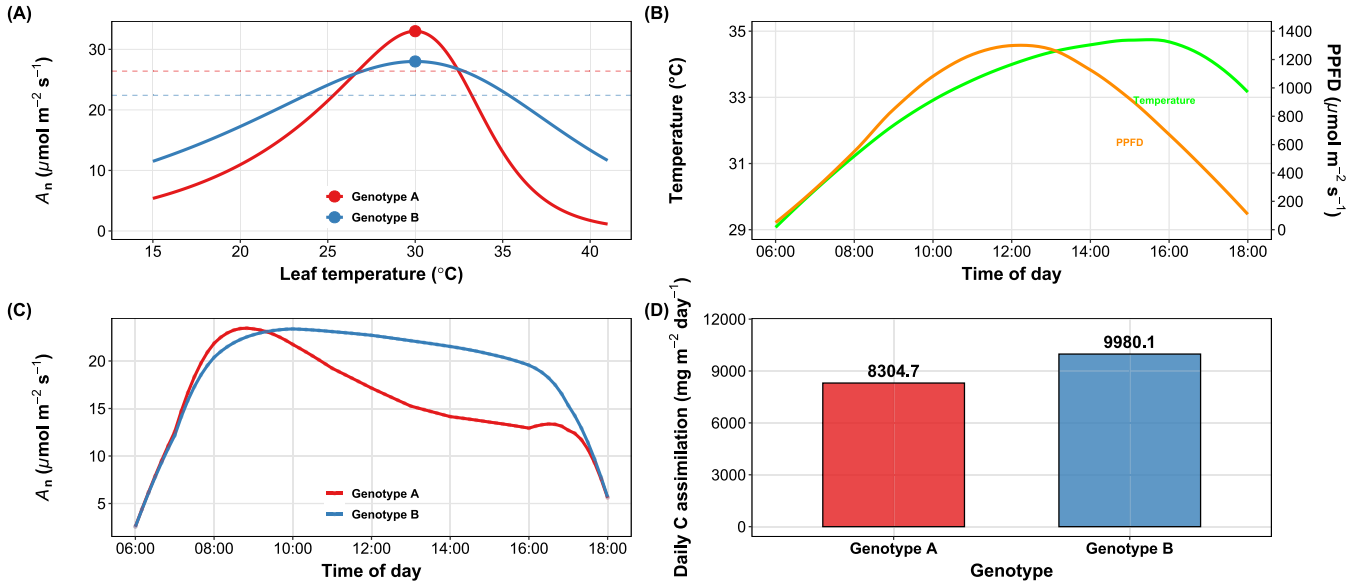

FIGURE 6 | Illustration of how temperature-response curve shape influences daily carbon assimilation. (A) Two representative thermal response curve types, a sharp, peak-shaped curve (Genotype A) and a broad, plateau-shaped curve (Genotype B). The two genotypes share similar A_{opt} but differ markedly in thermal breadth and high-temperature sensitivity. (B) Representative midsummer diurnal course of air temperature (green line) and photosynthetic photon flux density (PPFD; orange line) used for simulation. Environmental data were averaged at 10-min intervals across August 2025, in Wuhan. (C) Simulated diurnal photosynthetic rate (A_n) for the two genotypes under the environmental conditions shown in (B). (D) Daily carbon assimilation estimated by integrating A_n over the daytime period.

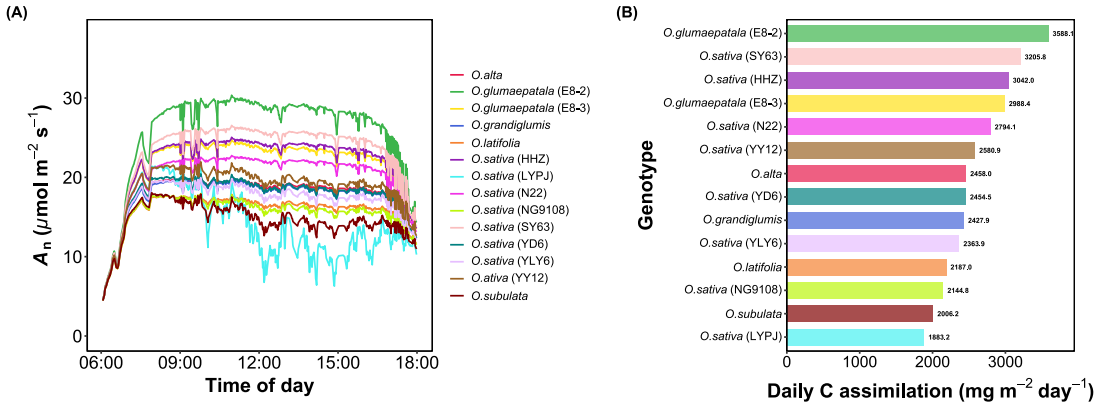

FIGURE 7 | Genotype-specific diurnal photosynthesis and daily carbon assimilation under a representative summer day. (A) Simulated diurnal photosynthetic rates (A_n) for 14 rice genotypes in a typical day in Wuhan, August 2025. Simulations incorporated each genotype's fitted temperature-response curve together with measured air temperature and PPFD recorded every 10 min. (B) Ranking of daily total carbon accumulation across the 14 genotypes. Genotypes are ordered vertically by their integrated daily carbon gain (mmol m^{-2} day^{-1}), calculated from the temporal integration of photosynthetic rates shown in (A).

by mechanistically separating the process into two key components: an activation term (E_a), driven by the kinetics of carboxylation and electron transport, and a deactivation term (D_s), associated with the thermal stability of key enzymes like Rubisco and membrane integrity (Scafaro et al. 2023; Sharkey 2005). Although other formulations may offer specific advantages for individual curves (Dusenge et al. 2025; Kontopoulos et al. 2024; Kumarathunge et al. 2019; Sun et al. 2023), this approach enabled systematic evaluation of shared and divergent thermal response traits.

The analysis demonstrated that peak-centered traits such as A_{opt} and T_{opt} alone did not reliably predict thermal performance under realistic conditions. Despite substantial differences in photosynthetic rates, T_{opt} remained relatively conserved, exhibiting the lowest phenotypic coefficient of variation among all measured traits (PCV = 5.7%). This limited variation is consistent with earlier evidence that T_{opt} shows strong physiological conservatism in C_3 species (Crous et al. 2024; Dusenge et al. 2021, 2025; Scafaro et al. 2019; Wittemann et al. 2022), likely constrained by the coordinated temperature dependencies of multiple, interdependent biochemical processes such as Rubisco kinetics, RuBP regeneration and thylakoid electron transport (Sage and Kubien 2007; Yamori et al. 2013), indicating that traditional peak metrics capture only a small portion of the underlying thermal diversity (Dowd et al. 2015; Dusenge et al. 2025).

In contrast, shape-based traits that describe performance stability showed markedly greater variation. The phenotypic coefficient of variation for the high-temperature sensitivity slope ($Slope_{higher}$) exceeded 70%, revealing that thermostability, the capacity to maintain photosynthetic function as temperatures rise above the optimum, is a highly variable and largely independent physiological dimension (Busch and Sage 2016; Scafaro et al. 2023; Wise et al. 2004). This high variability in thermostability may stem from genetic differences in mechanisms that protect the photosynthetic machinery from heat damage, such as the activity of Rubisco activase, the abundance of heat-shock proteins (HSPs), membrane lipid composition and antioxidant capacity (Mathur et al. 2014; Salvucci and Crafts-Brandner 2004; Sharkey 2005). Genotypes spanned a broad continuum in the trait space defined by thermal breadth (Breadth80) and overall temperature sensitivity, reflecting distinct thermal strategies within the rice gene pool (Chen et al. 2021; Hu et al. 2021; Jagadish et al. 2007; Liang et al. 2025; Zhang et al. 2023; Zhu et al. 2007). Genotypes such as HHZ, characterised by wide thermal breadth, and SY63, exhibiting low absolute sensitivity, highlight the availability of potentially valuable stability traits that remain underutilised in breeding programs (Briceño et al. 2025; Wang et al. 2021; Wu et al. 2016; Zhang, Feng, et al. 2022; Zhang et al. 2025). Notably, both HHZ and SY63 have been independently identified in previous research as exhibiting enhanced thermotolerance, with HHZ maintaining function over a wide temperature range and SY63 showing minimal yield decline under high temperature stress (Hu et al. 2024; Huang et al. 2016; Wang et al. 2021; Wu et al. 2017; Yang et al. 2017; Zhang et al. 2025).

4.2 | Curve-Shape Traits Reveal Alternative Thermal Strategies

The shape of the photosynthetic thermal response curve is an emergent property resulting from the interplay between activation E_a, reflecting processes that accelerate with warming (e.g., enzyme kinetics, electron transport) and deactivation D_s, reflecting processes that are destabilised by heat (e.g., enzyme denaturation, membrane leakiness). While thermal response curve shape determines how genotypes allocate photosynthetic capacity across the temperature range, and this allocation reflects distinct thermal strategies shaped by evolutionary history or breeding selection (Dusenge et al. 2025; Laza et al. 2015; Slot and Winter 2017; von Caemmerer and Evans 2014). Genotypes with broad thermal response curves, characterised by large Breadth80 values and shallow slopes, likely possess a combination of moderate activation energy and, crucially, a high tolerance to deactivation processes. This could be achieved through more thermostable protein complexes or enhanced repair mechanisms, allowing them to maintain relatively stable photosynthetic rates across a wide temperature range. Such thermally stable types appear less vulnerable to short-term departures from T_{opt}, a key advantage in environments where leaf temperatures routinely oscillate by 10°C or more within a day. In contrast, genotypes with narrow breadth and steep post-T_{opt} declines may have high activation energy driving a sharp peak, coupled with low resistance to deactivation. Their photosynthetic machinery, while potentially highly efficient at the optimum, is rapidly compromised upon heating, exhibiting sharp reductions in photosynthetic performance once temperatures exceeded the optimum. These thermally sensitive types may achieve high peak performance under controlled conditions but suffer disproportionately under realistic warming episodes (Lawas et al. 2018; Liu et al. 2025). Strategies for indica rice adapted to high-temperature stress in the middle and lower reaches of the Yangtze River.

The trait-space defined by Breadth80 and Slope traits revealed clear separation among genotypes, illustrating at least three broad thermal strategies (Zhang et al. 2023). First, broad-and-stable types, such as SY63 and N22, combined wide thermal breadth with low sensitivity, indicating robust photosynthetic performance under fluctuating temperatures. These traits align with the eurythermal curve type (Dowd et al. 2015), which confers stability in mean performance under thermal variability. This physiological stability likely stems from a balanced investment in both photosynthetic capacity and protective/repair mechanisms. Such a strategy enables sustained physiological function and productivity under warming conditions, as documented in prior studies (Wang et al. 2021; Wu et al. 2017; Wu et al. 2016; Zhang et al. 2023). Second, high-capacity but fragile types, exemplified by *O. glumaepatala* (E8-2), paired high A_{opt} with relatively steep post-T_{opt} sensitivity, suggesting enhanced productivity under benign conditions but reduced tolerance to heat stress. This pattern aligns with theoretical predictions that genotypes optimised for peak performance often have narrow, steeply declining thermal niches (Martin and Huey 2008; Vasseur et al. 2014), This suggests a physiological trade-off: resources are allocated primarily to maximise light-saturated photosynthesis, potentially at the expense of mechanisms that maintain system integrity under thermal stress. Consequently, such genotypes have a low thermal safety margin, a trait that may be maladaptive under increasing climate variability (Angilletta 2006; Dowd et al. 2015). Notably, similarly high photosynthetic capacity is observed in some wild rice species such as *O. australiensis* and *O. latifolia* (Mathan et al. 2021), suggesting that anatomical and biochemical adaptations enhancing light-saturated photosynthesis may coincidentally heighten sensitivity to supra-optimal temperatures. Third, heat-sensitive types, such as LYPJ, exhibited narrow thermal breadth and steep post-T_{opt} declines. This profile indicates a physiology characterised by both a constrained capacity for photosynthetic activation and poor defence against high-temperature deactivation, rendering it highly vulnerable. This inherent vulnerability aligns with the established heat susceptibility and severe yield reductions documented for this genotype (Hu et al. 2021, 2024; Wu et al. 2016). This stenothermal-like curve architecture explains its amplified performance loss under temperature variability (Dowd et al. 2015) and heightened vulnerability in fluctuating thermal environments. These physiological strategies arose independently of peak metrics, supporting the notion that thermal stability represents a distinct physiological axis. The dissociation between peak capacity and curve shape highlights the trade-offs governing thermal performance; genotypes optimised for high photosynthetic maxima often do so at the expense of stability, whereas those with moderate peaks may achieve superior cumulative carbon gain due to sustained performance across variable temperatures.

4.3 | Daily Carbon Gain Integrates Curve Traits

To reveal how curve shape, not just peak capacity, ultimately determines performance under realistic environmental conditions, we conducted simple carbon gain simulation analysis using instantaneous thermal response curve parameters. When exposed to a representative midsummer diurnal temperature pattern, genotypes with plateau-like curves sustained relatively high photosynthetic rates across morning and afternoon periods, even as temperatures deviated from T_{opt}. This sustained performance is a direct functional manifestation of the broad-and-stable physiological strategy described above. By contrast, peak-shaped curves, despite exhibiting higher A_{opt}, showed rapid declines once temperatures rose above the optimum, resulting in a shorter duration of high photosynthetic activity and reduced daily carbon gain.

These dynamics were clearly reflected in the genotype-specific simulations. *O. glumaepatala* (E8-2), for example, achieved the highest daily carbon gain, not solely because of its high A_{opt} but because its moderate thermal breadth allowed photosynthesis to remain effective throughout much of the day. This genotype demonstrates that a moderately high A_{opt}, when coupled with sufficient breadth, can be advantageous. However, its relatively high sensitivity suggests this advantage might be precarious under more extreme or prolonged heatwaves. In contrast, LYPJ accumulated the least carbon despite not having the lowest A_{opt}. Its narrow thermal breadth and steep post-T_{opt} sensitivity caused photosynthesis to decline sharply during the hottest hours (Angilletta 2006; Dowd et al. 2015), demonstrating how even a genotype with reasonable peak performance can be disadvantaged under fluctuating high temperatures. This discrepancy reveals a critical pitfall in traditional phenotyping: strategies that select solely for performance at a single optimal temperature or even for A_{opt} alone are liable to identify genotypes whose performance collapses under the variable conditions of the field.

Across all genotypes, daily carbon gain in naturally fluctuating environments is shaped more critically by thermal breadth (Breadth80) and slope-based sensitivity than by peak photosynthetic capacity (A_{opt}), supporting the idea that cumulative productivity depends on maintaining function over time rather than maximising short-term photosynthetic rates. However, carbon assimilation alone does not capture the full complexity of heat tolerance. It must be considered alongside other critical traits, such as reproductive-stage heat tolerance to ensure comprehensive stress adaptation. This finding shifts the focus from 'peak efficiency' to 'integrated resilience', a paradigm more aligned with the challenges posed by climate change (Vasseur et al. 2014). This result has important implications for breeding strategies. Selecting for high A_{opt} alone may inadvertently favour genotypes that are vulnerable to heat-induced declines, particularly as warming trends intensify and extreme temperature events become more frequent (Chopra et al. 2025; Padilla et al. 2025; Zhang, He, et al. 2022). Instead, curve-shape traits, particularly wide thermal breadth and low high-temperature sensitivity, should be emphasised as key indicators of resilience. We propose that these shape-based traits, derived from standardised models like the modified Arrhenius, offer a scalable, physiologically informative phenotyping toolkit for breeding programs aimed at climate resilience.

5 | Conclusion

In this study, we demonstrate that rice genotypes exhibit substantial diversity in their photosynthetic temperature responses, but that this diversity is only weakly captured by traditional peak traits such as T_{opt} and A_{opt}. In contrast, curve-shape traits describing thermal breadth and high-temperature sensitivity revealed a wide spectrum of thermal strategies that more accurately reflect how photosynthesis performs under fluctuating field conditions. Daily carbon-gain simulations further showed that thermal stability, rather than peak capacity, plays a dominant role in determining cumulative productivity during hot summer conditions. These findings highlight thermostability as a distinct and underutilised physiological dimension in rice and underscore the importance of incorporating curve-shape traits into future phenotyping and breeding programs. By targeting genotypes with broad thermal operating ranges and reduced high-temperature sensitivity, rice improvement efforts can better meet the challenges posed by climate warming.

Author Contributions

Dongliang Xiong and Qiaoyun Zhang planned and designed the research; Qiaoyun Zhang and Sheng Liang performed the experiments; Qiaoyun Zhang conducted data analyses with guidance from Dongliang Xiong and Liang Fang; Qiaoyun Zhang wrote the paper with inputs from Dongliang Xiong, Liang Fang, Xianke Yang and Xiaoxia Ling.

Acknowledgements

The authors thank Mr. Sheng Liang for his help in conducting photosynthetic temperature response measurements. We are grateful to the National Field Genebank for Wild Rice (Guangzhou, Guangdong) for providing the wild rice germplasm used in this study. AI disclosure statement: We confirm our full compliance with the journal and Wiley's policy on the use of artificial intelligence (AI) in scholarly writing. During the preparation of this manuscript, AI tools were used in a limited and assistive manner for two specific purposes: (1) assisting with R code writing for figure generation, and (2) polishing a small number of sentences to improve clarity during the revision process. No AI tools were used in research design, data collection, data analysis, interpretation of results or generation of scientific conclusions. For AI- assisted code, all R code was carefully reviewed, tested and validated by the authors. The output figures were checked against the original data to ensure accuracy and reproducibility. For language edits, all AI- suggested revisions were reviewed and evaluated by the authors, with final wording chosen based on scientific judgement to ensure accurate representation of the research. The research design, data collection, data analysis, scientific interpretation and core scientific writing were carried out by the authors. AI was used only as a productivity tool for coding and occasional language refinement. The authors take full responsibility for the entire manuscript, including all AI- assisted content.

Funding

The study is supported by Key Research and Development Program of Hubei Province (2023BBB037) and the China Agriculture Research System (CARS-01-24).

Consent

The corresponding authors had the consent of all co-authors before submitting the article for publication.

Conflicts of Interest

The authors declare no conflicts of interest.

Data Availability Statement

Data available on request from the authors.

References

Acevedo-Siaca, L. G., R. Coe, W. P. Quick, and S. P. Long. 2021. "Evaluating Natural Variation, Heritability, and Genetic Advance of Photosynthetic Traits in Rice (*Oryza sativa*)." *Plant Breeding* 140: 745–757.

Angilletta, M. J. 2006. "Estimating and Comparing Thermal Performance Curves." *Journal of Thermal Biology* 31: 541–545.

Asbury, D. A., and M. J. Angilletta Jr. 2010. "Thermodynamic Effects on the Evolution of Performance Curves." *American Naturalist* 176: E40–E49.

Atkin, O. K., I. Scheurwater, and T. L. Pons. 2006. "High Thermal Acclimation Potential of Both Photosynthesis and Respiration in Two Lowland Plantago Species in Contrast to an Alpine Congeneric." *Global Change Biology* 12: 500–515.

Bernacchi, C. J., C. Pimentel, and S. P. Long. 2003. "In Vivo Temperature Response Functions of Parameters Required to Model RuBP-Limited Photosynthesis." *Plant, Cell and Environment* 26: 1419–1430.

Briceño, V. F., P. A. Arnold, A. M. Cook, et al. 2025. "Drivers of Thermal Tolerance Breadth of Plants Across Contrasting Biomes." *Journal of Ecology* 113: 3812–3829.

Busch, F., N. P. A. Hüner, and I. Ensminger. 2007. "Increased Air Temperature During Simulated Autumn Conditions Does Not Increase Photosynthetic Carbon Gain but Affects the Dissipation of Excess Energy in Seedlings of the Evergreen Conifer Jack Pine." *Plant Physiology* 143: 1242–1251.

Busch, F. A., and R. F. Sage. 2016. "The Sensitivity of Photosynthesis to O_2 and CO_2 Concentration Identifies Strong Rubisco Control Above the Thermal Optimum." *New Phytologist* 213: 1036–1051.

Bytnerowicz, T. A., P. R. Akana, K. L. Griffin, and D. N. L. Menge. 2022. "Temperature Sensitivity of Woody Nitrogen Fixation Across Species and Growing Temperatures." *Nature Plants* 8: 209–216.

Cai, C., G. Li, L. Di, et al. 2020. "The Acclimation of Leaf Photosynthesis of Wheat and Rice to Seasonal Temperature Changes in T-FACE Environments." *Global Change Biology* 26: 539–556.

Carter, A. L., B. L. Bodensteiner, J. B. Iverson, et al. 2019. "Breadth of the Thermal Response Captures Individual and Geographic Variation in Temperature-Dependent Sex Determination." *Functional Ecology* 33: 1928–1939.

Chen, L., Q. Wang, M. Tang, et al. 2021. "QTL Mapping and Identification of Candidate Genes for Heat Tolerance at the Flowering Stage in Rice." *Frontiers in Genetics* 11: 621871.

China Meteorological Administration (CMA). 2024. China Climate Bulletin 2023. Beijing: China Meteorological Press.

Chopra, P., N. Sapia, O. Karami, et al. 2025. "Priming Thermotolerance: Unlocking Heat Resilience for Climate-Smart Crops." *Philosophical Transactions of the Royal Society, B: Biological Sciences* 380: 20240234.

Coast, O., B. C. Posch, H. Bramley, et al. 2021. "Acclimation of Leaf Photosynthesis and Respiration to Warming in Field-Grown Wheat." *Plant, Cell and Environment* 44: 2331–2346.

Crous, K. Y., K. B. Middleby, A. W. Cheesman, et al. 2024. "Leaf Warming in the Canopy of Mature Tropical Trees Reduced Photosynthesis due to Downregulation of Photosynthetic Capacity and Reduced Stomatal Conductance." *New Phytologist* 245: 1421–1436.

Deng, Z. R., S. W. Zhou, M. R. Wang, et al. 2023. "Changes in the Midsummer Extreme High-Temperature Events Over the Yangtze River Valley Associated With the Thermal Effect of the Tibetan Plateau and Arctic Oscillation." *Atmospheric Research* 293: 106911.

Dowd, W. W., F. A. King, M. W. Denny, J. E. Podrabsky, J. H. Stillman, and L. Tomanek. 2015. "Thermal Variation, Thermal Extremes and the Physiological Performance of Individuals." *Journal of Experimental Biology* 218: 1956–1967.

Du, T., P. Meng, J. Huang, S. Peng, and D. Xiong. 2020. "Fast Photosynthesis Measurements for Phenotyping Photosynthetic Capacity of Rice." *Plant Methods* 16: 6.

Dusenge, M. E., S. González-Caro, Z. Restrepo, et al. 2025. "Unexpected Large Photosynthetic Thermal Plasticity of Montane Andean Trees." *Global Change Biology* 31: e70266.

Dusenge, M. E., M. Wittemann, M. Mujawamariya, et al. 2021. "Limited Thermal Acclimation of Photosynthesis in Tropical Montane Tree Species." *Global Change Biology* 27: 4860–4878.

Galmés, J., M. V. Kapralov, L. O. Copolovici, C. Hermida-Carrera, and Ü. Niinemets. 2015. "Temperature Responses of the Rubisco Maximum Carboxylase Activity Across Domains of Life: Phylogenetic Signals, Trade-Offs, and Importance for Carbon Gain." *Photosynthesis Research* 123: 183–201.

Geange, S. R., P. A. Arnold, A. A. Catling, et al. 2020. "The Thermal Tolerance of Photosynthetic Tissues: A Global Systematic Review and Agenda for Future Research." *New Phytologist* 229: 2497–2513.

Glaubitz, U., X. Li, K. I. Koehl, J. T. van Dongen, D. K. Hincha, and E. Zuther. 2014. "Differential Physiological Responses of Different Rice (*Oryza sativa*) Cultivars to Elevated Night Temperature During Vegetative Growth." *Functional Plant Biology* 41: 437–448.

Gong, W., C. Proud, S. Fukai, and J. Mitchell. 2023. "Low Canopy Temperature and High Stomatal Conductance Contribute to High Grain Yield of Contrasting *Japonica* Rice Under Aerobic Conditions." *Frontiers in Plant Science* 14: 1176156.

Hu, Q. Q., W. C. Wang, Q. F. Lu, J. L. Huang, S. B. Peng, and K. H. Cui. 2021. "Abnormal Anther Development Leads to Lower Spikelet Fertility in Rice (*Oryza sativa* L.) Under High Temperature During the Panicle Initiation Stage." *BMC Plant Biology* 21: 428.

Hu, Q. Q., N. Yan, K. H. Cui, et al. 2024. "Increased Panicle Nitrogen Application Improves Rice Yield by Alleviating High-Temperature Damage During Panicle Initiation to Anther Development." *Physiologia Plantarum* 176: e14230.

Huang, L., Y. Sun, S. Peng, and F. Wang. 2016. "Genotypic Differences of Japonica Rice Responding to High Temperature in China." *Agronomy Journal* 108: 626–636.

Jagadish, S. V. K., P. Q. Craufurd, and T. R. Wheeler. 2007. "High Temperature Stress and Spikelet Fertility in Rice (*Oryza sativa* L.)." *Journal of Experimental Botany* 58: 1627–1635.

Jagadish, S. V. K., M. V. R. Murty, and W. P. Quick. 2014. "Rice Responses to Rising Temperatures—Challenges, Perspectives and Future Directions." *Plant, Cell & Environment* 38: 1686–1698.

Jiang, M., Z. Chen, Y. Li, X. Huang, L. Huang, and Z. Huo. 2024. "Rice Canopy Temperature Is Affected by Nitrogen Fertilizer." *Journal of Integrative Agriculture* 23: 824–835.

Jiang, M., K. Guo, J. Wang, Y. Wu, X. Shen, and L. Huang. 2023. "Current Status and Prospects of Rice Canopy Temperature Research." *Food and Energy Security* 12: e424.

Kanno, K., T. Mae, and A. Makino. 2009. "High Night Temperature Stimulates Photosynthesis, Biomass Production and Growth During the Vegetative Stage of Rice Plants." *Soil Science and Plant Nutrition* 55: 124–131.

Katahata, S. I., Q. Han, M. Naramoto, Y. Kakubari, and Y. Mukai. 2014. "Seasonal Changes in Temperature Response of Photosynthesis and

Its Contribution to Annual Carbon Gain in *Daphniphyllum humile*, an Evergreen Understorey Shrub." *Plant Biology* 16: 345–353.

Kontopoulos, D. G., A. Sentis, M. Daufresne, N. Glazman, A. I. Dell, and S. Pawar. 2024. "No Universal Mathematical Model for Thermal Performance Curves Across Traits and Taxonomic Groups." *Nature Communications* 15: 8855.

Kumarathunge, D. P., B. E. Medlyn, J. E. Drake, et al. 2019. "Acclimation and Adaptation Components of the Temperature Dependence of Plant Photosynthesis at the Global Scale." *New Phytologist* 222: 768–784.

Lawas, L. M. F., W. Shi, M. Yoshimoto, et al. 2018. "Combined Drought and Heat Stress Impact During Flowering and Grain Filling in Contrasting Rice Cultivars Grown Under Field Conditions." *Field Crops Research* 229: 66–77.

Laza, M. R. C., H. Sakai, W. Cheng, T. Tokida, S. Peng, and T. Hasegawa. 2015. "Differential Response of Rice Plants to High Night Temperatures Imposed at Varying Developmental Phases." *Agricultural and Forest Meteorology* 209: 69–77.

Li, L., T. Ding, H. Gao, and Z. Ke. 2025. "Entire-Basin Heat Wave in the Yangtze River Is Becoming the New Normal." *Journal of Applied Meteorology and Climatology* 64: 761–775.

Liang, S. F., W. P. Liu, M. Lu, et al. 2025. "Climate Adaptation Through Rice Northward Expansion Aggravated Groundwater Overexploitation in Northeast China." *Communications Earth & Environment* 6: 516.

Liu, C., B. Sun, G. Wang, et al. 2018. "Effects of Open Temperature Increasing on Photosynthesis and Chlorophyll Fluorescence Parameters of Japonica Rice." *Ecology and Environmental Sciences* 27: 1665–1672.

Liu, L., C. Yuan, Y. Chen, et al. 2024. "RICE-HDM: A Remote Sensing Framework for Monitoring Rice High-Temperature Heat Damage in the Middle and Lower Reaches of the Yangtze River." In *3rd International Conference on Frontiers of Artificial Intelligence and Machine Learning (FAIML)*, 347–351. Coll Comp & Informat Tech.

Liu, Z. Q., D. P. Xu, R. L. Wang, et al. 2025. "Effects of Temperature Fluctuations on the Growth Cycle of Rice." *Agriculture* 15: 99.

Makino, A. 2021. "Photosynthesis Improvement for Enhancing Productivity in Rice." *Soil Science and Plant Nutrition* 67: 513–519.

Martin, T. L., and R. B. Huey. 2008. "Why 'Suboptimal' Is Optimal: Jensen's Inequality and Ectotherm Thermal Preferences." *American Naturalist* 171: E102–E118.

Mathan, J., A. Singh, V. Jathar, and A. Ranjan. 2021. "High Photosynthesis Rate in Two Wild Rice Species Is Driven by Leaf Anatomy Mediating High Rubisco Activity and Electron Transport Rate." *Journal of Experimental Botany* 72: 7119–7135.

Mathur, S., D. Agrawal, and A. Jajoo. 2014. "Photosynthesis: Response to High Temperature Stress." *Journal of Photochemistry and Photobiology B: Biology* 137: 116–126.

Medlyn, B. E., E. Dreyer, D. Ellsworth, et al. 2002. "Temperature Response of Parameters of a Biochemically Based Model of Photosynthesis. II. A Review of Experimental Data." *Plant, Cell & Environment* 25: 1167–1179.

Molnár, P. K., J. P. Sckrabulis, K. A. Altman, and T. R. Raffel. 2017. "Thermal Performance Curves and the Metabolic Theory of Ecology—A Practical Guide to Models and Experiments for Parasitologists." *Journal of Parasitology* 103: 423–439.

Moore, C. E., K. Meacham-Hensold, P. Lemonnier, et al. 2021. "The Effect of Increasing Temperature on Crop Photosynthesis: From Enzymes to Ecosystems." *Journal of Experimental Botany* 72: 2822–2844.

Noguchi, K., W. Yamori, K. Hikosaka, and I. Terashima. 2015. "Homeostasis of the Temperature Sensitivity of Respiration Over a Range of Growth Temperatures Indicated by a Modified Arrhenius Model." *New Phytologist* 207: 34–42.

Padfield, D., H. O'Sullivan, and S. Pawar. 2021. "rTPC and Nls. Multstart: A New Pipeline to Fit Thermal Performance Curves in r." *Methods in Ecology and Evolution* 12: 1138–1143.

Padilla, Y., V. Fotopoulos, G. Ntatsi, et al. 2025. "Strategies for Enhancing Resilience in Horticultural Crops Against Combined Abiotic Stresses." *Physiologia Plantarum* 177: e70502.

Radhakrishna, N. K. A., V. Chenniappan, and V. Dhashnamurthi. 2018. "Combined Effects of Drought and Moderately High Temperature on the Photosynthesis, PS II Photochemistry and Yield Traits in Rice (*Oryza sativa* L.)." *Indian Journal of Plant Physiology* 23: 408–415.

Rehmani, M. I. A., C. Q. Ding, G. H. Li, et al. 2021. "Vulnerability of Rice Production to Temperature Extremes During Rice Reproductive Stage in Yangtze River Valley, China." *Journal of King Saud University* 33: 101599.

Rohr, J. R., D. J. Civitello, J. M. Cohen, E. A. Roznik, B. Sinervo, and A. I. Dell. 2018. "The Complex Drivers of Thermal Acclimation and Breadth in Ectotherms." *Ecology Letters* 21: 1425–1439.

R Core Team. 2022. A language and environment for statistical computing. R Foundation for Statistical Computing, Vienna, Austria. https://www.R-project.org/.

Sage, R. F., and D. S. Kubien. 2007. "The Temperature Response of C3 and C4 Photosynthesis." *Plant, Cell & Environment* 30: 1086–1106.

Salvucci, M. E., and S. J. Crafts-Brandner. 2004. "Inhibition of Photosynthesis by Heat Stress: The Activation State of Rubisco as a Limiting Factor in Photosynthesis." *Physiologia Plantarum* 120: 179–186.

Sang, Y. F. 2012. "Spatial and Temporal Variability of Daily Temperature in the Yangtze River Delta, China." *Atmospheric Research* 112: 12–24.

Scafaro, A. P., N. Bautsoens, B. den Boer, J. Van Rie, and A. Gallé. 2019. "A Conserved Sequence From Heat-Adapted Species Improves Rubisco Activase Thermostability in Wheat." *Plant Physiology* 181: 43–54.

Scafaro, A. P., B. C. Posch, J. R. Evans, G. D. Farquhar, and O. K. Atkin. 2023. "Rubisco Deactivation and Chloroplast Electron Transport Rates Co-Limit Photosynthesis Above Optimal Leaf Temperature in Terrestrial Plants." *Nature Communications* 14: 2820.

Sharkey, T. D. 2005. "Effects of Moderate Heat Stress on Photosynthesis: Importance of Thylakoid Reactions, Rubisco Deactivation, Reactive Oxygen Species, and Thermotolerance Provided by Isoprene." *Plant, Cell & Environment* 28: 269–277.

Sharkey, T. D., and R. Zhang. 2010. "High Temperature Effects on Electron and Proton Circuits of Photosynthesis." *Journal of Integrative Plant Biology* 52: 712–722.

Shi, W., X. Yin, P. C. Struik, et al. 2017. "High Day- and Night-Time Temperatures Affect Grain Growth Dynamics in Contrasting Rice Genotypes." *Journal of Experimental Botany* 68: 5233–5245.

Slot, M., and K. Winter. 2017. "In Situ Temperature Response of Photosynthesis of 42 Tree and Liana Species in the Canopy of Two Panamanian Lowland Tropical Forests With Contrasting Rainfall Regimes." *New Phytologist* 214: 1103–1117.

Song, X., G. Wang, B. Sun, et al. 2019. "Effects of Free Air Temperature Increasing on Photosynthesis and Yield of Japonica Rice With Different Heat-Tolerance Characteristics." *Journal of Shenyang Agricultural University* 50: 648–655.

Sun, T., X. Zhang, S. Lv, et al. 2023. "Improving the Predictions of Leaf Photosynthesis During and After Short-Term Heat Stress With Current Rice Models." *Plant, Cell & Environment* 46: 3353–3370.

Vasseur, D. A., J. P. DeLong, B. Gilbert, et al. 2014. "Increased Temperature Variation Poses a Greater Risk to Species Than Climate Warming." *Proceedings of the Royal Society B: Biological Sciences* 281: 20132612.

von Caemmerer, S., and J. R. Evans. 2014. "Temperature Responses of Mesophyll Conductance Differ Greatly Between Species." *Plant, Cell & Environment* 38: 629–637.

Wang, W. C., K. H. Cui, Q. Q. Hu, et al. 2021. "Response of Spikelet Water Status to High Temperature and Its Relationship With Heat Tolerance in Rice." *Crop Journal* 9: 1344–1356.

Way, D. A., and R. F. Sage. 2008. "Elevated Growth Temperatures Reduce the Carbon Gain of Black Spruce *Picea mariana* (Mill.) BSP." *Global Change Biology* 14: 624–636.

Way, D. A., and W. Yamori. 2013. "Thermal Acclimation of Photosynthesis: On the Importance of Adjusting Our Definitions and Accounting for Thermal Acclimation of Respiration." *Photosynthesis Research* 119: 89–100.

Wise, R. R., A. J. Olson, S. M. Schrader, and T. D. Sharkey. 2004. "Electron Transport Is the Functional Limitation of Photosynthesis in Field-Grown Pima Cotton Plants at High Temperature." *Plant, Cell & Environment* 27: 717–724.

Wittemann, M., M. X. Andersson, B. Ntirugulirwa, L. Tarvainen, G. Wallin, and J. Uddling. 2022. "Temperature Acclimation of Net Photosynthesis and Its Underlying Component Processes in Four Tropical Tree Species." *Tree Physiology* 42: 1188–1202.

Wu, C., K. Cui, W. Wang, et al. 2017. "Heat-Induced Cytokinin Transportation and Degradation Are Associated With Reduced Panicle Cytokinin Expression and Fewer Spikelets Per Panicle in Rice." *Frontiers in Plant Science* 8: 371.

Wu, C., K. H. Cui, W. C. Wang, et al. 2016. "Heat-Induced Phytohormone Changes Are Associated With Disrupted Early Reproductive Development and Reduced Yield in Rice." *Scientific Reports* 6: 34978.

Xu, J., A. Henry, and N. Sreenivasulu. 2020. "Rice Yield Formation Under High Day and Night Temperatures—A Prerequisite to Ensure Future Food Security." *Plant, Cell and Environment* 43: 1595–1608.

Yamasaki, T., T. Yamakawa, Y. Yamane, H. Koike, K. Satoh, and S. Katoh. 2002. "Temperature Acclimation of Photosynthesis and Related Changes in Photosystem II Electron Transport in Winter Wheat." *Plant Physiology* 128: 1087–1097.

Yamori, W., K. Hikosaka, and D. A. Way. 2013. "Temperature Response of Photosynthesis in C3, C4, and CAM Plants: Temperature Acclimation and Temperature Adaptation." *Photosynthesis Research* 119: 101–117.

Yamori, W., K. O. Noguchi, and I. Terashima. 2005. "Temperature Acclimation of Photosynthesis in Spinach Leaves: Analyses of Photosynthetic Components and Temperature Dependencies of Photosynthetic Partial Reactions." *Plant, Cell & Environment* 28: 536–547.

Yang, Y., Q. Zhang, G. Huang, S. Peng, and Y. Li. 2020. "Temperature Responses of Photosynthesis and Leaf Hydraulic Conductance in Rice and Wheat." *Plant, Cell and Environment* 43: 1437–1451.

Yang, Y. J., M. Y. Zhang, Q. X. Li, et al. 2020. "Modulations of Surface Thermal Environment and Agricultural Activity on Intraseasonal Variations of Summer Diurnal Temperature Range in the Yangtze River Delta of China." *Science of the Total Environment* 736: 139445.

Yang, Z. Y., Z. L. Zhang, T. Zhang, et al. 2017. "The Effect of Season-Long Temperature Increases on Rice Cultivars Grown in the Central and Southern Regions of China." *Frontiers in Plant Science* 8: 1908.

Yin, X. 2021. "No Need to Switch the Modified Arrhenius Function Back to the Old Form." *New Phytologist* 231: 2113–2116.

Yin, X., and P. C. Struik. 2017. "Can Increased Leaf Photosynthesis Be Converted Into Higher Crop Mass Production? A Simulation Study for Rice Using the Crop Model GECROS." *Journal of Experimental Botany* 68: 2345–2360.

Zhang, M., K. Feng, X. Dong, et al. 2022. "Screening of Heat-Tolerant Indica Rice Varieties in the Middle and Lower Yangtze River." *Agronomy-Basel* 12: 2462.

Zhang, M., Z. Li, K. Feng, et al. 2023. "Strategies for Indica Rice Adapted to High-Temperature Stress in the Middle and Lower Reaches of the Yangtze River." *Frontiers in Plant Science* 13: 1081807.

Zhang, S. Q., Y. Y. Ren, G. Y. Ren, and S. K. Tysa. 2025. "The Change and Urbanization Effect on Extreme Temperature Trends in the Yangtze River Basin." *Theoretical and Applied Climatology* 156: 22.

Zhang, T. Y., Y. He, R. DePauw, et al. 2022. "Climate Change May Outpace Current Wheat Breeding Yield Improvements in North America." *Nature Communications* 13: 5591.

Zhu, S. Q., C. M. Yu, X. Y. Liu, B. H. Ji, and D. M. Jiao. 2007. "Changes in Unsaturated Levels of Fatty Acids in Thylakoid PSII Membrane Lipids During Chilling-Induced Resistance in Rice." *Journal of Integrative Plant Biology* 49: 463–471.

Supporting Information

Additional supporting information can be found online in the Supporting Information section. **Figure S1:** Modulating the photosynthetic temperature response curve by varying activation energy (E_a) and deactivation entropy (D_s) parameters in the modified Arrhenius model. Simulated curves illustrate the individual and combined effects of the two key thermodynamic parameters. All curves share fixed values for the optimal temperature ($T_{opt} = 30°C$) and maximum photosynthetic rate (A_{opt} at $30\,\mu mol\,m^{-2}s^{-1}$). Red group (constant $D_s = 200\,kJ\,mol^{-1}$): The black solid curve ($E_a = 100\,kJ\,mol^{-1}$) serves as a common reference. Decreasing E_a to $40\,kJ\,mol^{-1}$ (thin red line) flattens the initial rise, while increasing E_a to $70\,kJ\,mol^{-1}$ (medium red line) steepens it. Blue group (constant $E_a = 100\,kJ\,mol^{-1}$): The same black solid curve ($D_s = 200\,kJ\,mol^{-1}$) is used as the reference. Increasing D_s to $300\,kJ\,mol^{-1}$ (medium blue line) or $400\,kJ\,mol^{-1}$ (thin blue line) progressively broadens the decline after the optimum and reduces the peak rate. **Figure S2:** Variation in key photosynthetic thermal parameters across the 14 rice genotypes. **Figure S3:** Relationships among key photosynthetic thermal adaptation traits. (A) Hierarchical clustering. The dendrogram groups traits based on their similarity in response patterns across genotypes, revealing two primary clusters: one associated with photosynthetic performance (e.g., A_{opt}, $Slope_{lower}$) and another with thermal stability (e.g., T_{opt}, Breadth80, $Slope_{higher}$). (B) Correlation matrix. Pairwise Pearson correlations between all traits are shown. Red and blue colours indicate positive and negative correlations, respectively. Asterisks denote statistical significance (* represents $p < 0.05$, ** represents $p < 0.01$; *** represents $p < 0.001$). **Figure S4:** Diurnal patterns of air temperature and photosynthetic photon flux density (PPFD) on a representative hot day. Measured environmental conditions (air temperature and PPFD) from 06:00 to 18:00 h on 18 August 2025. This diurnal profile served as the key environmental input for the subsequent simulation of photosynthetic performance. **Figure S5:** Diurnal variation in net photosynthetic rate (A_n) for rice genotypes representing the extremes of daily carbon gain (top three vs. bottom three). Net photosynthetic rate (A_n) is shown across a representative day. Lines depict the top three genotypes (solid lines) and bottom three genotypes (dashed lines) ranked by their total daily carbon gain. Each colour represents a distinct genotype. **Table S1:** List of the 14 rice accessions used in this study, selected based on their contrasting heat tolerance and genetic diversity. **Table S2:** Differences in net photosynthetic rate (ΔA_n) and linear response slopes across consecutive leaf temperature intervals. **Table S3:** Fitted parameters of leaf photosynthetic temperature response curves for the 14 rice genotypes. **Table S4:** Functional traits of photosynthetic temperature response for 14 rice genotypes derived from the Modified Arrhenius model. The table summarises the key shape-based functional traits calculated from the Modified Arrhenius model fits. Breadth80 and Breadth50 represent the thermal performance breadth at 80% and 50% of A_{opt}, respectively. $Slope80_{lower}$ and $Slope50_{lower}$ denote the temperature sensitivity slopes from the lower boundary (T_{lower}) of Breadth80 or Breadth50 to T_{opt}, while $Slope80_{higher}$ and $Slope50_{higher}$ represent the corresponding slopes from T_{opt} to the upper boundary (T_{higher}). $Slope\_ratio_{80}$ and $Slope\_ratio_{50}$ quantify the asymmetry of temperature sensitivity by calculating $Slope_{lower}/Slope_{higher}$ at their respective thresholds. Composite is the performance stability index, calculated as $A_{opt} \times$ Breadth80. These traits form the basis for the strategic classification and stability evaluation in this study.